

Fig 1 Yaw angle as a function of time, comparing the approximate solution with a numerical solution of the differential equation

Defining a nondimensional time

$$\tau = 1 + t/T_b$$

reduces the equation to

$$\varphi'' + 2KT_b\varphi' + K_1^2V_0^2T_b^2\tau^2\varphi = 0 \quad (5)$$

where the prime denotes differentiation with respect to  $\tau$ . By letting

$$\varphi(\tau) = e^{-KT_b\tau}\theta(\tau)$$

the first derivative in Eq (5) is removed, giving

$$\theta'' + K_1^2V_0^2T_b^2(-K^2/K_1^2V_0^2 + \tau^2)\theta = 0 \quad (6)$$

For the size of rocket studied, a representative value of  $(K/K_1V_0)^2$  is  $(3/V_0)^2$ , where  $V_0$  is the initial velocity in feet per second. Since the smallest value of  $\tau$  is one, the factor  $(3/V_0)^2$  may be neglected if the rocket has an appreciable initial velocity. In the numerical computation, the rocket was given an initial velocity of 600 mph, and hence the factor  $(3/V_0)^2$  is neglected. In this case, Eq (6) becomes

$$\theta'' + K_1V_0^2T_b^2\tau^2\varphi = 0 \quad (7)$$

The solution to Eq (7) is given in terms of Bessel Functions:

$$\theta = C\tau^{1/2}J_{1/4}(\frac{1}{2}K_1V_0T_b\tau^2) + D\tau^{1/2}Y_{1/4}(\frac{1}{2}K_1V_0T_b\tau^2)$$

where the constants  $C$  and  $D$  are determined from the initial conditions. The solution for yaw is, therefore,

$$\varphi(t) = \tau^{1/2}e^{-KT_b\tau}[CJ_{1/4}(\frac{1}{2}K_1V_0T_b\tau^2) + DY_{1/4}(\frac{1}{2}K_1V_0T_b\tau^2)] \quad (8)$$

Assuming an initial velocity such that  $K_1V_0T_b\tau^2 > 10$ , the argument of the Bessel Functions becomes large enough to allow approximation by trigonometric functions. For the rockets studied, the factor  $K_1V_0T_b\tau^2$  ranged from 10-40 for an initial velocity of 600 mph. In this case,

$$\varphi(t) = C_1\tau^{-1/2}e^{-KT_b\tau}\cos(\frac{1}{2}K_1V_0T_b\tau^2 - D_1) \quad (9)$$

where  $C_1$  and  $D_1$  are determined from the initial conditions. Equation (9) exhibits, in closed form, the property that the amplitude of the oscillation decreases as the factor  $\tau^{-1/2}e^{-KT_b\tau}$ , and that the frequency increases proportionally to the nondimensional time.

In Fig 1 the approximation given by Eq (9) is compared to a numerical solution of the original equation for yaw [Eq (3)] demonstrating that Eq (9) is a satisfactory approximation for the case studied.

#### Reference

- 1 Rosser, J. B., Newton, R. R., and Gross, G. L., *Mathematical Theory of Rocket Flight* (McGraw-Hill Book Co., Inc., New York 1947) p. 20.

## Magnetohydrodynamic Hypersonic Viscous Flow Past a Blunt Body

MYRON C. SMITH\*

*The Rand Corporation, Santa Monica, Calif*

AND

CHING-SHENG WU†

*Jet Propulsion Laboratory,  
California Institute of Technology, Pasadena, Calif*

In this paper the equations governing the hypersonic flow about a magnetized body are solved numerically. The solutions obtained illustrate the effects of Reynolds number and magnetic parameter on the structure of the applied magnetic field. The results show that, for magnetic parameters larger than a critical value, numerical solutions do not exist. A critical magnetic parameter is considered to result from an assumption of a given magnetic field at the shock. By increasing the conductivity, and thereby the induced magnetic field, the applied field at the shock disappears. This, in turn, violates the basic assumption of a finite field at the shock. It is concluded that the applied magnetic field can only be defined at the body where it is a natural characteristic of the problem.

#### Introduction

THE mathematical complexity of the problem of hypersonic flow about a magnetized body is great even if the investigation is restricted to the local similarity solutions. For computational simplification, Bush and Wu investigated the problem by considering the given magnetic field strength at the shock wave.<sup>1,2</sup> Bush found that numerical integration becomes impossible for the inviscid case when the value of the magnetic parameter exceeds a certain critical value. This paper extends Wu's study of the viscous case<sup>2</sup> to a much wider range of the parameters by using digital computer techniques. Computational difficulties similar to those found by Bush were encountered. This paper will report some results and at the same time provide a physical interpretation for the nonexistence of numerical solutions for magnetic parameters higher than the critical value, which depends upon the value of the viscous Reynolds number.

#### Local-Similarity Solution

The assumptions used here are those used in Ref. 2. The vehicle is assumed to be moving at a speed (Mach > 15) sufficient to cause a significant amount of shock ionization of the gas behind the detached shock wave. In addition, the fluid is assumed to be incompressible, viscous, and in steady state. The applicable equations are as follows:

$$\nabla \cdot \mathbf{v} = 0$$

$$\nabla \times [(\nabla \times \mathbf{v}) \times \mathbf{v} - (\mu_e/4\pi\rho)(\nabla \times \mathbf{H}) \times \mathbf{H}] = \nu \nabla^2 \nabla \times \mathbf{v} \quad (1)$$

$$\nabla \cdot \mathbf{H} = 0$$

$$\nabla \times [\nabla \times \mathbf{H} - 4\pi\sigma\mu_e\mathbf{v} \times \mathbf{H}] = 0$$

Received February 13, 1964. This research is sponsored by the U. S. Air Force under Project RAND. Views or conclusions contained in this paper should not be interpreted as representing the official opinion or policy of the U. S. Air Force. The authors are indebted to R. E. Kalaba and H. Kagiwada of the Rand Corporation for the mathematical techniques and difficult computer program.

\* Physical Scientist, Electronics Department

† Senior Scientist

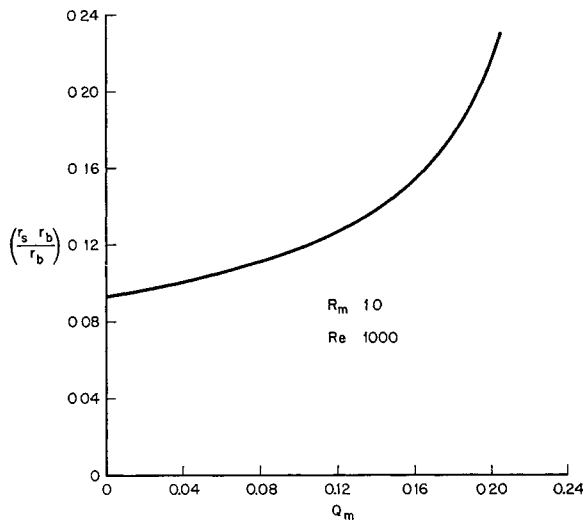


Fig 1 Standoff distance vs magnetic parameter

where

- $\mu$  = magnetic permeability
- $\sigma$  = electrical conductivity
- $\mathbf{H}$  = magnetic field intensity
- $\nu$  = kinematic viscosity
- $\nabla^2$  = Laplacian operator
- $\mathbf{v}$  = velocity vector
- $\rho$  = density

The spherical body is assumed to contain a dipole magnetic field axisymmetric with the flow field. The postulated similarity solutions associated with the stagnation-point flow have the following functional form:

$$\begin{aligned} v &= v_\infty [2f(\eta)/\eta^2] \cos\theta \\ v_\theta &= -v_\infty [(1/\eta)(df/d\eta)] \sin\theta \\ H &= H_0 [2g(\eta)/\eta^2] \cos\theta \\ H_\theta &= -H_0 [(1/\eta)(dg/d\eta)] \sin\theta \end{aligned} \quad (2)$$

where the angle  $\theta$  is measured from the axis of symmetry,  $v_\infty$  and  $H_0$  are the freestream velocity and reference dipole magnetic field, respectively, and  $\eta = r/r_s$  ( $r_s$  = shock radius).

From Eqs (1) and (2), using a right-handed spherical coordinate frame with  $\sin\theta \simeq \frac{1}{2} \sin 2\theta$

$$f \frac{d}{d\eta} \left[ \frac{1}{\eta^2} \left( \frac{2f}{\eta^2} - \frac{d^2f}{d\eta^2} \right) \right] - M_p g \frac{d}{d\eta} \left[ \frac{1}{\eta^2} \left( \frac{2g}{\eta^2} - \frac{d^2g}{d\eta^2} \right) \right] = \frac{1}{2Re} \left[ \left( \frac{1}{\eta} \frac{d}{d\eta} \frac{\eta^2 d}{d\eta} - \frac{2}{\eta} \right) \left( \frac{2f}{\eta^3} - \frac{1}{\eta} \frac{d^2f}{d\eta^2} \right) \right] \quad (3)$$

and the induction equation becomes

$$\frac{2g}{\eta^2} - \frac{d^2g}{d\eta^2} = 2R_m \left[ g \frac{df}{d\eta} - f \frac{dg}{d\eta} \right] \frac{1}{\eta^2} \quad (4)$$

where

- $M_p = \mu H_0^2 / 4\pi \rho_\infty v_\infty^2$  = magnetic pressure number
- $R_m = 4\pi \sigma \mu v_\infty r_s$  = magnetic Reynolds number
- $Q_m = M_p R_m$  = magnetic parameter
- $Re = v_\infty r_s / \nu$  = Reynolds number

#### Boundary Conditions at the Shock

Equations (3) and (4) are solved satisfying boundary conditions at the surface of the body as well as directly behind the shock wave. The conditions at the shock are based on the continuity of flow and the magnetic field. The former gives

$$f(1) = -(\epsilon/2) \quad (df/d\eta)_{\eta=1} = -1 \quad (5)$$

and the latter gives

$$g(1) = 1 \quad (dg/d\eta)_{\eta=1} = -1 \quad (6)$$

where  $\epsilon = \rho_\infty / \rho$ , the ratio of density across the shock. The other boundary condition at the shock is based on the vorticity jump, i.e.,

$$\left( \frac{d^2f}{d\eta^2} \right)_{\eta=1} = 2 - 2\epsilon - \frac{1}{\epsilon} - 4 \frac{Q_m}{\epsilon} \left( 1 + \frac{\epsilon}{2} \right) \quad (7)$$

The magnetic field was specified on the shock [Eq (6)] rather than at the body surface to simplify the mathematical solution.

#### Boundary Conditions at the Body

The flow is governed at the body by the condition of non-slip and zero radial velocity

$$f(\eta_b) = 0 \quad (df/d\eta)_{\eta=\eta_b} = 0 \quad (8)$$

where  $\eta_b = r_b/r$ , and  $r_b$  is the radius of the body.

#### Computation Procedure

A quasi-linearization technique was used in the solution of the two-point boundary value problem. The solution consisted of solving ordinary differential Eqs (3) and (4), satisfying, simultaneously, five conditions on the shock and two conditions on the body. Since the shock standoff distance is also unknown, a transformation to independent variable  $t$

$$\eta = [(\eta_b/\eta) - 1]t + 1 \quad (9)$$

gives the integration range  $0 \leq t \leq 1$ , where the standoff distance  $\zeta (= \eta_b/\eta - 1)$  is an unknown. The differential equation

$$d\zeta/dt = 0 \quad (10)$$

is added to Eqs (3) and (4). Equations (3, 4, and 9) reduce to a set of seven first-order ordinary differential equations and seven boundary conditions. The initial value of  $\zeta$  is determined by the boundary conditions. The quasi-linearization solution scheme is described in Ref 3.

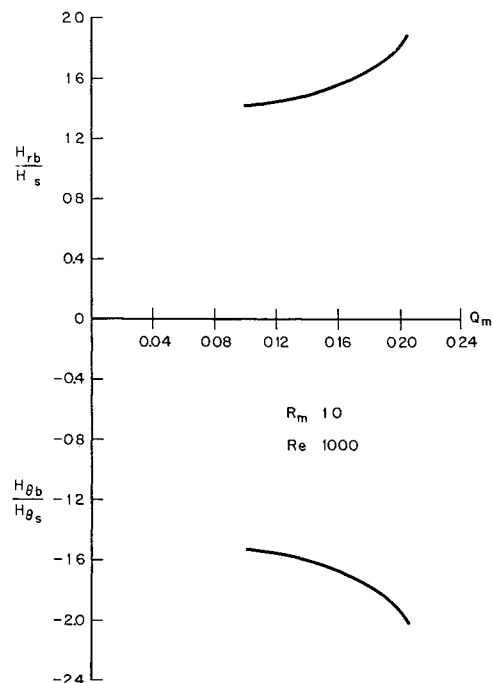


Fig 2 Magnetic field at the body vs magnetic parameter

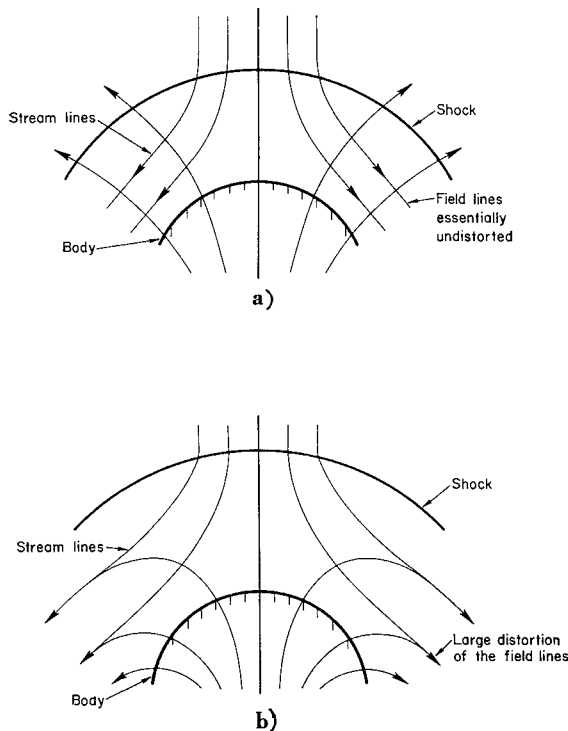


Fig 3 Magnetic field lines for a) small conductivity and b) large conductivity

#### Discussion of Results

A plot of the standoff distances and  $Q_m$  in Fig 1 indicates that, when the value of  $Q_m$  exceeds 0.20 (for  $Re = 1000$ ,  $R_m = 1.0$ ), the quantity  $(r - r_b)/r_b$  increases drastically, so that

$$d/dQ_m[(r - r_b)/r_b] \rightarrow \infty$$

Because of this phenomenon, the numerical solution for the case  $Q_m$  greater than the critical value mentioned previously becomes impossible. Similar difficulty was also observed by Bush<sup>1</sup>. The meaning of the critical  $Q_m$  was first pointed out by Bush<sup>4</sup> in a note published after Ref 1. He has shown that, if we accept the result of infinitely large shock standoff distance, the finite value of critical  $Q_m$  implies an infinitely strong magnetic field at the body. This can be seen from the plot given in Fig 2 where the magnetic field components at the body are plotted as a function of the magnetic parameter.

To assume that the magnetic field is given at the shock does give considerable mathematical simplification, but evidently for high conductivity the solution obtained by using this boundary condition no longer represents the physical problem. This fact can be realized by considering the weakly conducting case ( $\sigma \rightarrow 0$ ) and the infinitely conducting case ( $\sigma \rightarrow \infty$ ). The magnetic field lines for these cases are shown in Figs 3a and 3b. In the case ( $\sigma \rightarrow 0$ ), the applied dipole field is essentially not distorted (Fig 3a). However, where ( $\sigma \rightarrow \infty$ ) the distortion of the field lines becomes so large that the field strength at the shock wave vanishes (Fig 3b). This situation violates the basic assumption of a field  $H_0$  at the shock.

Another flaw of the present method is that since  $r$  and  $H_0$  at the shock, are not natural characteristic quantities of the problem, a plot of these quantities vs  $Q_m$ ,  $R_m$ , and  $Re$  is not quite meaningful. An improved method of approach is underway and will be reported later.

#### References

- <sup>1</sup> Bush, W. B., "Magnetohydrodynamic-hypersonic flow past a blunt body," *J. Aerospace Sci.* **25**, 685-690, 728 (November 1958).
- <sup>2</sup> Wu, C. S., "Hypersonic viscous flow near the stagnation

point in the presence of a magnetic field," *J. Aerospace Sci.* **27**, 882-893, 950 (December 1960).

<sup>3</sup> Bellman, R., Kagiwada, H., and Kalaba, R. E., "Orbit determination as a multi-point boundary value problem and quasilinearization," *Proc. Natl. Acad. Sci.* **48**, 1327-1329 (1962).

<sup>4</sup> Bush, W. B., "A note on magnetohydrodynamic hypersonic flow past a blunt body," *J. Aerospace Sci.* **26**, 536-537 (1959).

## Determination of Cratering Energy Densities for Metal Targets by Means of Reflectivity Measurements

HERMAN MARK,\* GARY GOLDBERG,†

AND MICHAEL J. MIRTICH†

NASA Lewis Research Center, Cleveland, Ohio

ANY attempt to estimate the lifetime of satellites or satellite components exposed to the high-speed meteoroid environment in the vicinity of the earth requires information in two areas. First, knowledge is required of the damage to a structure surface resulting from an encounter with a single meteoroid (if not the understanding of all the complex phenomena that occur during such an impact). Then, reliable information is required regarding the number of encounters with meteoroids of different size, speed, and composition which can be expected to occur in a given time in orbit. Unfortunately, for the satellite lifetime estimates, information in both these areas is either unsatisfactory or lacking. The work reported herein was undertaken to determine the damage to surface optical properties due to exposure to impact with high-speed micron-size particles and thus to contribute some information in the first area previously mentioned.

Polished aluminum surfaces were bombarded by clouds of high-speed SiC particles having an average diameter of  $6 \mu$ . The number, size, and velocity of the particles was either known or measured, and with the total kinetic energy of the cloud characterizing the exposure, changes in reflectivity of the exposed surfaces were measured with an infrared spectrometer. A good correlation of the measured reflectivity, before and after exposure, was obtained with the equation<sup>1</sup>

$$\bar{\rho}_f = \bar{\rho}_i \{1 - [1 - (\bar{\rho}_\infty/\bar{\rho}_i)](1 - e^{-K_1 \epsilon})\} \quad (1)$$

where

$\bar{\rho}_f$  = average final reflectivity of area  $A_0$  after exposure to  $\epsilon$

$\bar{\rho}_i$  = average initial reflectivity of area  $A_0$ , (0.97 for polished Al)

$\bar{\rho}_\infty$  = average reflectivity after infinite exposure, (0.15 for target assumed coated with projectile material)

$K_1$  = empirical constant, 0.229/joule falling on  $A_0$

$\epsilon = \sum_{i=1}^N \frac{1}{2} m_i v_i^2$ , total kinetic energy of particle cloud falling on area  $A_0$ , joules

In the development of this equation, it becomes clear that the constant  $K_1$  is the percentage of fresh area damaged per unit impact energy. With the assumption that hemispherical shaped craters are formed on impact,<sup>2</sup>  $K_1$  is related to  $E_c$ ,

Received January 20, 1964

\* Chief, Aero-Space Environment Branch, Associate Fellow Member AIAA

† Aerospace Engineer, Space Environment Section